JOURNAL OF MATERIALS SCIENCE **39** (2004) 5711–5717

Preliminary analysis of pore distributions using NMR in natural coral and hydrothermally prepared hydroxyapatite

A. L. McCUTCHEON, G. S. KAMALI KANNANGARA, M. A. WILSON*
Office of the Dean, College of Science Technology and Environment, University of Western, Sydney Locked Bag 1797, Penrith South DC, NSW 1797, Australia
E-mail: ma.wilson@uws.edu.au

B. BEN-NISSAN
Department of Chemistry, Materials and Forensic Science, University of Technology, Sydney PO. Box 123, Broadway, NSW 2007, Australia

Pore size distributions in an Australian coral from *Goniopora sp* have been measured by mercury intrusion, nuclear magnetic resonance (NMR) and scanning electron microscopy (SEM). A significant result is that NMR predicts nanopores which could be seen visibly. The methods give similar results as mercury intrusion for large pores around 100 μm but differ for smaller pores. Differences between NMR and mercury intrusion are equated using a non linear sigmoidal regression model. The NMR method was also compared with mercury intrusion methods to measure pore sizes on hydroxyapatite conversion products which have promise as bio-implants. Differences between samples due to errors in the methodology are discussed. Together all three methods are shown to complement each other.

1. Introduction

A range of methods can be used to measure pore sizes in porous materials. Each of these methods has their drawbacks. Gas adsorption and desorption techniques are only suitable for measuring mesopores with diameters less than 20 nm. On the other hand visual inspection of cross sections is useful normally only for larger pores. Moreover if the pores are irregular or heterogeneous in their geometry, a cross section can be misleading. Multi-point mercury injection porosimetry does not suffer these problems, although it tends to reflect pore throats not pore sizes, and damage and pore size alteration can occur in friable materials particularly to nanopores or nanopores may not fill because they are too small or not interconnected [1].

Nuclear magnetic resonance also has its problems even though it can readily give data on friable material [2–8]. Nuclear magnetic resonance methods rely on the fact that when disturbed from its natural thermal energy by irradiation, a proton may diffuse across a pore enclosure filled with liquid water, and relax to a lower energy state by transferring magnetisation to the pore surface boundary. If the pore has small dimensions there is a high probability that the protons will collide with surface boundary or walls of the pore and relax. Thus on average, for a collection of protons, the average relaxation time is shorter in small pores compared with large pores and depends only on the pore size and its relaxation properties. Thus

$$T_1 = V/S\rho \quad \text{or} \quad 1/T_1 = S\rho/V \tag{1}$$

where V is the volume of the pore, S is the surface of the pore and ρ is a constant dependent on the surface, termed surface relaxitivity. This is the ability of the surface to cause relaxation and has the dimensions of length/time. Since the pore size is characterised (inter alia) by the surface (S) to volume ratio (V) as S/V NMR can be used to measure pore sizes. NMR measurements correlate with S/V measured by nitrogen adsorption studies. For mobile liquids such as water where molecular re-orientation is fast T_1 is equal to T_2 and hence T_2 is also related to pore size and can be substituted for T_1 in Equation 1 [9].

The essence of the NMR method is that S/V can be related to spin lattice relaxation (T_1) or spin spin relaxation (T_2). T_2 is the preferred measurement since it can be measured rapidly by the Carr-Purcell sequence [9]. The problem with nuclear magnetic resonance however is that relaxation can be caused by surface paramagnetics. That is, the surface relaxivity can vary in different parts of the sample. Moreover, if multiple pore types are present there are often a number of mathematical solutions which may not accurately portray pore size.

*Author to whom all correspondence should be addressed.

In this paper we make comparisons of pore size distributions by visual, mercury injection and relaxation methods on a coral to develop methodology and use this on its hydroxapatite conversion products. Some of these materials are particularly fragile and another method rather than mercury porosity would be desirable [10–16].

Alternate bio compatible materials such as monophasic hydroxyapatite have been used as bone grafts in an attempt to overcome the limitations of natural bone graft materials which often have insufficient strength [10–16]. Monophasic hydroxyapatite, can be synthesized from coral providing a material similar to the mineral content of teeth and bone [10–16]. Studies indicate that pore size and microstructural composition are important factors facilitating in-growth of fibrovascular tissue or bone from the host during grafting and hence strength. Hence more detailed analyses on pores are needed to understand the binding and strengthening process. Coral hydroxyapatite has been characterized using optical and electron microscopy and scanning electron microscopy, and mercury injection porosimetry, however details of pores structure are sketchy and we are unaware of any NMR porosity studies.

2. Experimental

The coral sample was from *Goniopora sp* and was obtained from the Great Barrier Reef (Australia). The coral samples were prepared by washing in 5% sodium hypochlorite solution followed by boiling in water to remove the bleaching agent. A sample of this coral weighing 45.95 g had a volume of 38 cm^3 which was determined by the displacement of cold water and confirmed measuring the dimensions of the sample. It absorbed 15.4 cm^3 of water when immersed in boiling water giving a porosity of 40.5%. The calculated bulk density is 1.21 g cm^{-3}.

Hydroxyapatite samples were prepared from washed coral by reaction in a Parr reactor (300 ml) Parr Instrument company USA equipped with a Teflon liner [10–13]. The reaction was carried out at 250°C with excess (2–3 times by weight) ammonium monohydrogen phosphate and water (150 ml) for 36 h. Pressure was kept at 3.8 MPa. The product hydroxyapatite was washed with water extensively, to remove excess ammonium monohydrogen phosphate and dried at 70°C and then fired in air at 500–900°C to fix the solution derived hydroxyapatite on the surface of corraline hydroxyapatite thus to cover the very small pores and to leave open the larger pores [17].

These samples were characterized whole as below.

2.1. Mercury porosimeter measurements

Pore distributions in both coral and hydroxyapatite sample were measured by mercury porosimetry on a Shimadzu Micrometrics Poresizer 9310. Results are reported with pore volume, differentially measured, as a function of pore dimension. The measured pressure, forcing mercury into the pores, was converted into a pore dimension using the Washburn equation [1]

$$r = \frac{-2\gamma\ \mathrm{Cos}\theta}{P} \tag{2}$$

where r is the pore radius, P is the pressure applied to force mercury into the pore, γ is the surface tension (480 mJ cm^{-2}) and θ is the contact angle (140°).

2.2. Image analyses using scanning electron microscopy

Using scanning electron microscopy (SEM) technique, images of the Australian coral sample were generated by employing a Jeol 6300F FEG SEM operated at 30 KV or a LEO SUPRA55VP, SEM. SEM images were generated to determine the pore size distribution, on a 5.6 × 3.9 mm portion of the coral face. The latter microscope is a field emission SEM with variable pressure capabilities. The microscope was operated at either 1 or 2 KV accelerating voltage at a working distance of 7 mm with the samples un-coated. Eight random images were recorded using one face of the C1 coral sample.

Images were processed to increase their contrast and produce bi-tonal images using Adobe image software. The boundary of the pores was determined where the image gradient was a maximum. Pores were counted and their dimensions were measured using Scion Image for Windows Release Beta 4 0 2 software. The software counts the pore radius minimum cases where the pore shape was not circular. Typical SEM data for the coral is given in Fig. 1a–c. We were only ably to get quantitative SEM data on the larger pores 40–140 μm pores. However Fig. 1b and c clearly shows smaller pores are present.

2.3. Nuclear magnetic resonance measurements

The porous samples were saturated with water by immersion in boiling water for at least half an hour. Proton nuclei relaxation processes were recorded on a Resonance Maran 2 broadline NMR spectrometer utilizing a large permanent magnet with a sample chamber of 13 cm diameter × 30 cm length—producing a low intensity field with a Larmor frequency of 2.1 MHz. The whole samples were enclosed in the chamber. The hydroxyapatite samples lost water rapidly and hence were wrapped in high density polyethylene (HDPE) to avoid water loss by evaporation from the sample during the analysis. The proton relaxation measurements were recorded, using the Carr-Purcell pulse sequence [9], with τ set to 150 μs, using 256 scans, a pulse length of 27.5 μs and a delay time of up to 10 s for the coral samples. The number of scans was increase to 16384 for the coral hydroxyapatite samples. After an initial $\pi/2$ pulse, a series of π pulses at τ, 3τ, 5τ, nτ μs etc. were applied to produce a series of echoes at 2τ, 4τ and 6τ etc. which decrease exponentially with time constant T_2. The effect of diffusion was kept minimal by keeping short the interval between the pulses so T_2

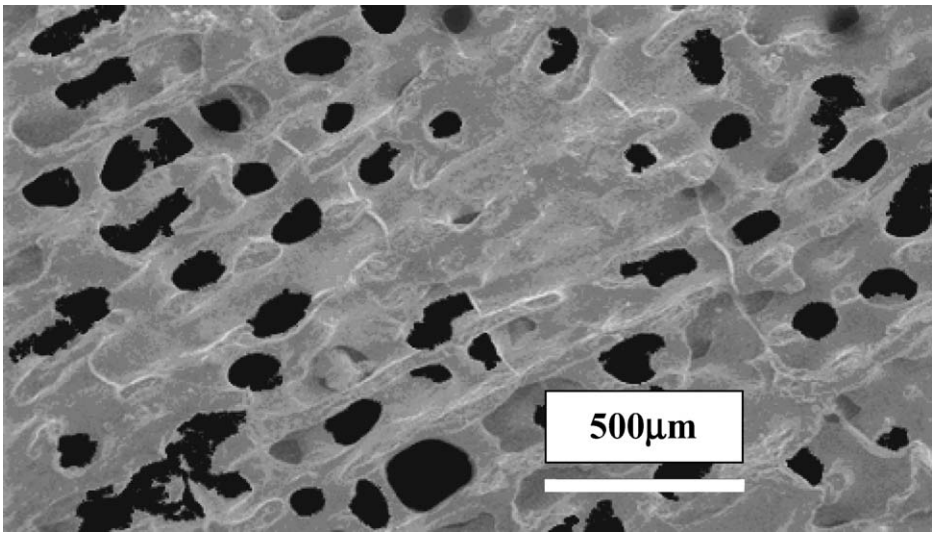

(a)

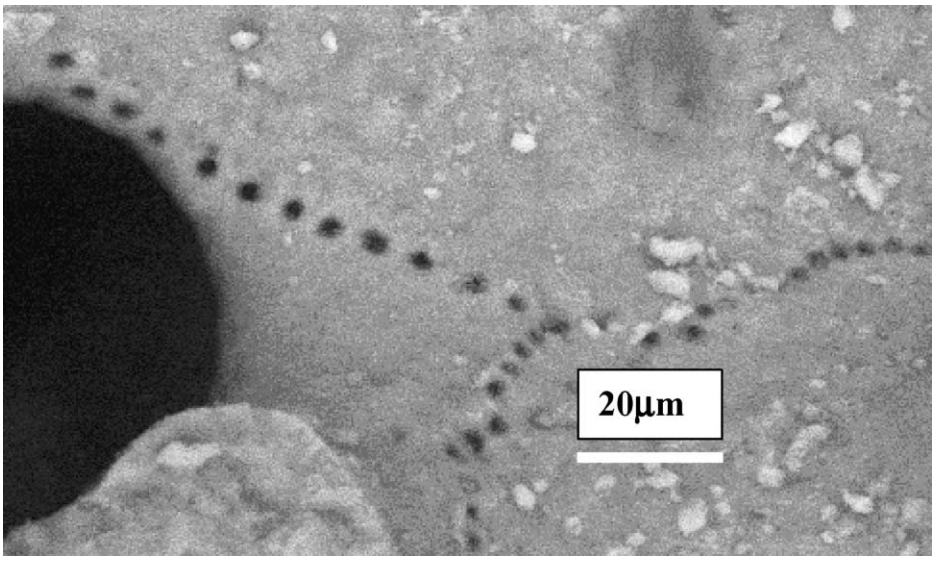

(b)

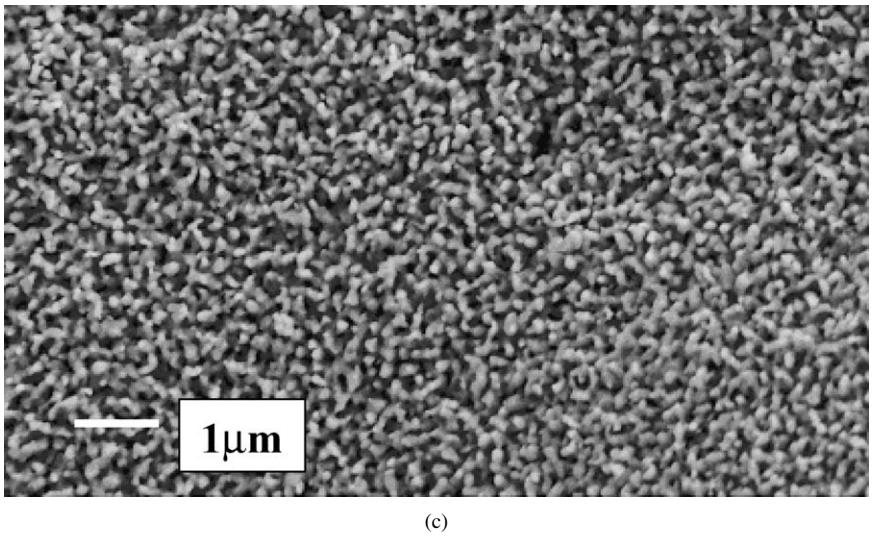

(c)

Figure 1 SEM image data for *Goniopora sp* coral, Images (a), (b) and (c) illustrate different pore sizes.

for each pore can be derived from the multiple simple Bloch equation [18–20] as:

$$M_t = \sum_i A_i \exp(-t/T_{2i}) \quad (3)$$

where A_i is a constant reflecting the contribution of each type of pore to the relaxation behaviour. In principle if T_{2i} values are known, pore size distributions can be measured by fitting values for M_t to obtain A_i [21–24] as amount A_i of pore characterised by T_{2i} which can

be calibrated as pore size i. Details of the relationship between pore size and T_2 are given elsewhere [8]. In practice, they are best fitted through integration over a continuous T_2 from values equal to zero to those for the bulk solution. In this data there is the presence of noise ε. Thus

$$M(t) = \int_{T_2=0}^{T_2 bulk} A(T_2 \exp(-t/T_2))d(T_2) + \varepsilon(t) \quad (4)$$

A values are interpreted as the number of pores if the pore geometry is known. T_2 is interpreted as pore size. To extract A values from this equation [23–25] weighting functions are applied with least squares minimisation techniques. The weighting functions used in this study are 0.0536 for the coral sample, 0.0865 and 0.0718 for the hydroxyapatite samples treated at 250 and 900°C respectively. Values of T_2 can be correlated by the simple relationship of Equation 1 if the constant ρ is known. For very small pores this can be done cryogenically, however here the pores are mostly large (ca. 100 microns) and they are too large to be determined using a freezing depression technique [8]. The behaviour of the hydroxyapatite surface is not known, thus the pores size was initially determined by overlaying the largest peak with that from porosity measurements and then a sigmoidal regression analysis was used to fit the data to the porosity data. This is discussed below.

3. Results and discussion

3.1. Coral samples

Large pores are present (Fig. 1a), on average around 100 μm but sometimes larger. The smallest pores around 1 μm (Fig. 1b) and others even smaller, <1 μm (Fig. 1c) are visible but not quantifiable. They are seen by NMR but not by mercury porosity. It seems likely the small pores are being destroyed by mercury intrusion.

TABLE I Parameters used in the Marquardt-Levenberg algorithm [25–27], applied to NMR T_2 data, enabling an optimum fit using different data sources

	MMF model parameters			
Compare NMR data with	a	b	c	d
Hg intrusion data for coral (C1)	2.62101	1.53×10^8	3213902	0.59467
Hg intrusion data for coral treated at 250°C	−0.03140	162118	135.589	0.92799
Hg intrusion data for coral treated at 900°C	−0.08555	1406838	677.018	0.92396

Typical NMR data for the *Goniopora sp* coral are given in Fig. 2 together with mercury porosity and visible data. To relate the NMR data to the mercury porosity data and the part of the visual data which can be quantified, a non linear sigmoidal regression model of the form

$$\text{Pore diam. } (\mu\text{m}) = \frac{ab + c \cdot (T_2)^{\text{d}}}{b + (T_2)^{\text{d}}} \quad (5)$$

was used. The parameters (Table I) of the model were adjusted, by iteration using the Marquardt-Levenberg algorithm [25–27], to obtain an optimum fit to the image data. This approach provided a very good fit between the two data sets, as illustrated in Fig. 3.

The visual image data that could be quantified is plotted in Fig. 4 with the iterated NMR data for the same pore region. There is not a complete fit and the image data is skewed to higher pore sizes. This is probably because the visual data does not include the small nano sized pores.

3.2. Hydroxyapatite samples

A range of different pores have been described on hydroxyapatite depending on preparation method [28].

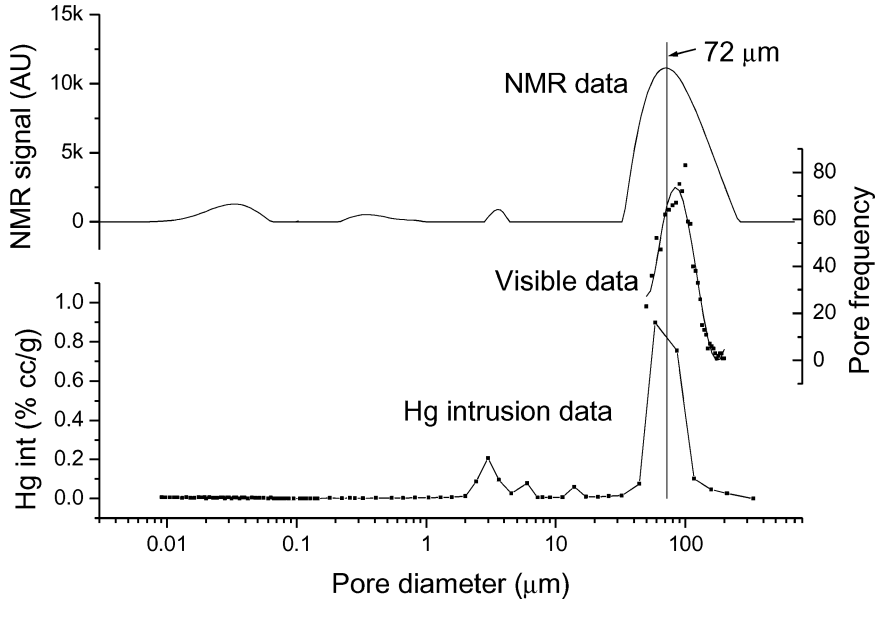

Figure 2 The NMR distribution data from *Goniopora sp* coral as a function of T_2 is plotted as a function of pore size. AU = absolute units and corresponds to volume/wt measure by mercury intrusion. A values are calculated from Equation 4 and interpreted as the number of pores of pore size determined by interpreting T_2 as pore size from Equation 1.

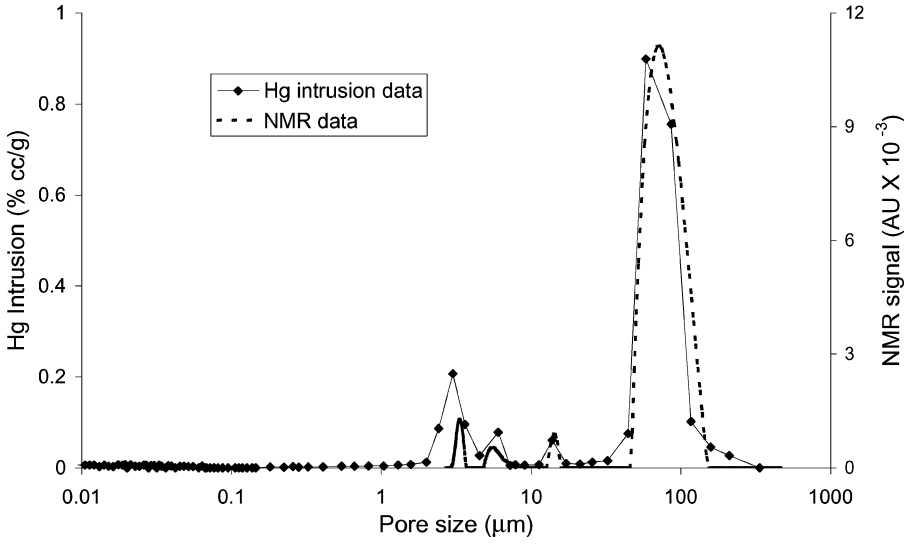

Figure 3 To correlate the NMR T_2 *Goniopora sp* coral data to pore size mercury intrusion data, the four modal peaks of the NMR data were matched and then the other data best fitted using Equation 5 by application of a sigmoidal reiterative process. AU = absolute units and corresponds to volume/wt measure by mercury intrusion.

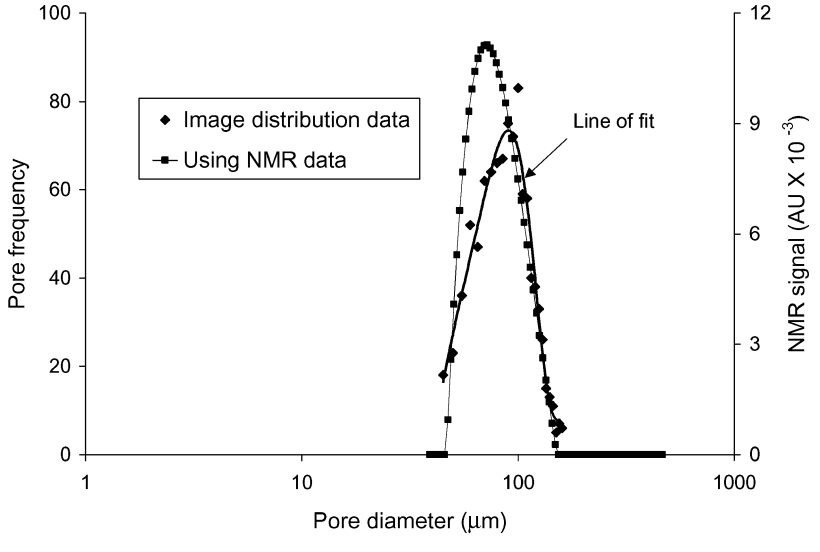

Figure 4 Visible data from *Goniopora sp* coral compared with NMR data, where the T_2's have been converted to pore size by application of a sigmoidal model using the Hg intrusion data as the reference. Note the x axis was maintained in the log form for consistency.

Studies on the conversion products are shown in Fig. 5. Mercury intrusion measurements show that reaction at 900°C appears to remove smaller pores around 1–3 μm and slightly increase the size of the larger pores. However the trends are small.

Figs 6 and 7 show that the NMR method suggests the same types of pores are present demonstrating the success of the method. However, the number of pores in each type differ because the mercury intrusion data cannot pick up many of the nanosized (0.1 μm) pores.

3.3. Nature of correlations

The above discussion assumes that the mercury intrusion data is in effect incorrect because it assumes nanopores are seen e.g., not destroyed or filled. However as mentioned in the introduction, this should be clarified since the NMR data also relies on assumption. The problem with extracting A values from Equation 4 which applies generically to all relaxation, including T_2 is that there are a wide set of values of A that adequately define the data. This type of problem is termed "ill posed". However, if the geometry of the structure in which the water is relaxing is known, then a single solution is possible. Thus Browstein and Tarr [23] modelled solutions for cylindrical and spherical geometries and confirmed their results using practical example of rat gastronemius cells. In assuming an annular cylindrical shape the model predicted the correct cell diameter. More recently, Prammer [24] showed that there are various ways to obtaining single solutions if weighting functions are applied with least squares minimisation techniques. In effect, this mathematically is a way of constricting the geometry. The fact that small, less than 1 μm pores were shown visibly for coral, there were good correlations and qualitatively NMR detected them, suggests the assumptions are valid. Indeed iteration using the Marquardt-Levenberg algorithm, allowed correlation with the mercury intrusion data. This is further illustrated by the hydroxyapatite sample and

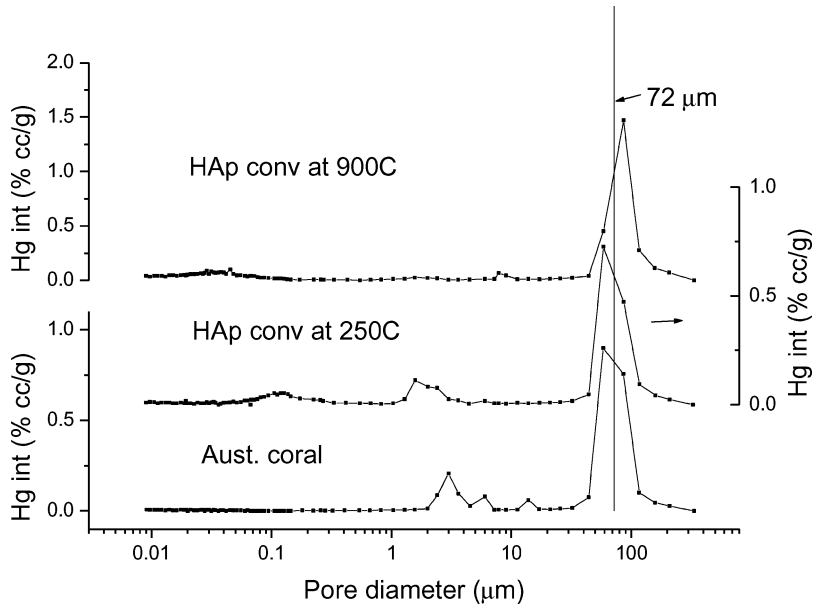

Figure 5 Mercury intrusion measurements for hydroxyapatites prepared at 250 and 900°C measurements for the Australian coral are included.

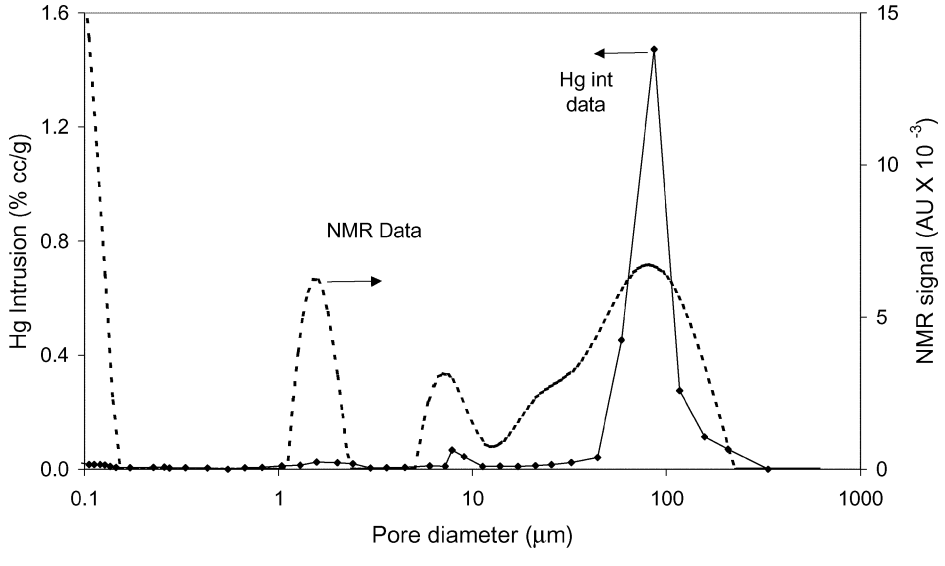

Figure 6 NMR and mercury intrusion data for hydroxyapatite prepared at 900°C .

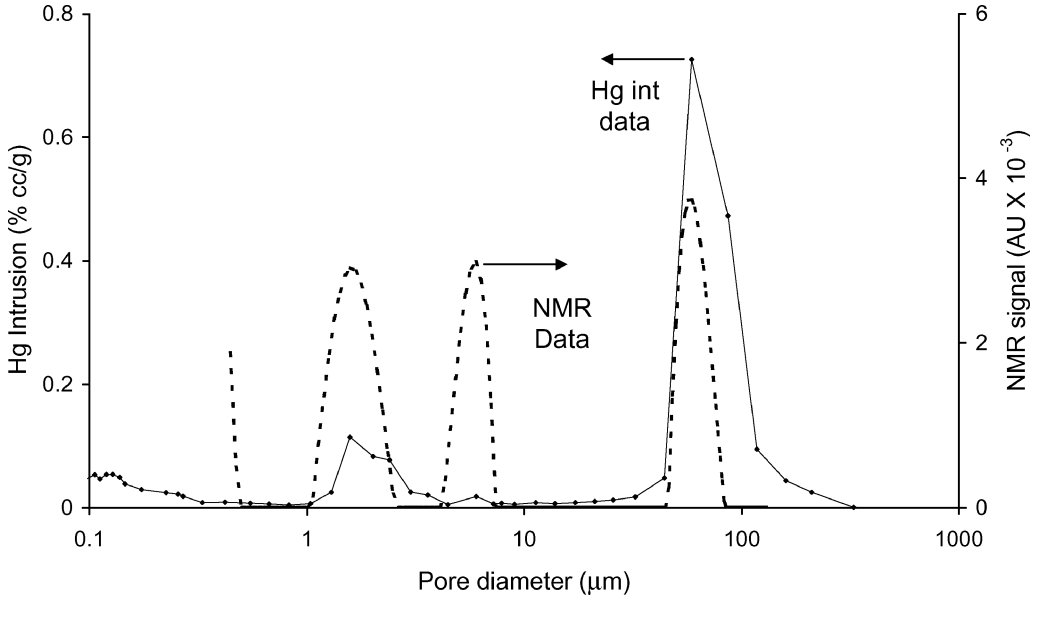

Figure 7 NMR and mercury intrusion data for hydroxyapatite prepared at 250°C.

supported by the differences between mercury intrusion and visible data, that the NMR method has promise for these samples.

It is clear from this work that the combination of three techniques for pore size measurements throws light on pore distribution which is not available from one technique alone. The NMR method does appear to provide useful comparative data and qualitatively indicate that other pores are present rather than those seen visibly. Bearing in mind the ease and rapid measurements by NMR it might be useful for comparing qualitatively coral samples which have fragility. After thermal treating of coral with excess ammonium monohydrogen phosphate the NMR data results suggest an increase in pore size in agreement with the mercury intrusion data. Further work is in progress to develop this into a direct imaging method. In magnetic resonance imaging a magnetic field gradient is placed across the sample so that T_2 values are a function of special distribution in the magnet as well as pore sizes.

Acknowledgments

The authors would like to thank A/Prof. A. Nakahira from Kyoto Institute of Technology, Japan for his contribution during the mercury porosimetry measurements aspects of this work. Financial support provided to Prof. Ben-Nissan by the Japan Society for the Promotion of Science (JSPS) under the JSPS/Australian Academy of Science Fellowship Program for Research in Japan scheme is also gratefully acknowledged.

References

1. S. LOWELL and J. E. SHIELDS, "Powder Surface Area and Porosity," 2nd ed. (Chapman and Hall, London, New York, 1984) p. 87.
2. J. KORRINGA, D. O. SEEVEERS and H. C. TORREY, *Phys. Rev.* **127** (1962) 1143.
3. H. A. RESING, J. K. THOMPSON and J. J. KREBS, *J. Phys. Chem.* **7** (1964) 1621.
4. A. TIMUR, *J. Petrol. Explor.* (1969) 775.
5. M. H. COHEN and K. S. MENDELSON, *J. Appl. Phys.* **53** (1982) 1127.
6. E. J. SCHMIDT, K. K. VELASCO and A. M. NUR, *ibid.* **59** (1986) 2788.
7. M. D. HURLIMAN, K. G. HELMER, L. L. LATLOUR and C. H. SOYAK, *J. Mag. Res. Series* A **111** (1994) 169.
8. A. L. McCUTCHEON, M. A. WILSON, B. HARTUNG-KAGI and O. KHIAM, *J. Phys. Chem.* **106** (2002) 2928.
9. H. Y. CARR and E. M. PURCELL, *Phys. Rev.* **94** (1954) 630.
10. B. BEN-NISSAN and G. PEZZOTTI, *J. Ceram. Soc. Jpn.* **110** (2002) 601.
11. J. H. KÜHNE, R. BARTL, B. FRISCH, C. HAMMER, V. JANSSON and M. ZIMMER, *Acta Orthopaedia Scandinavia* **65** (1994) 246.
12. J. HU, R. FRASER, J. J. RUSSELL, R. VAGO and B. BEN-NISSAN, *J. Mater. Sci. Technol.* **16** (2000) 591.
13. D. M. ROY and S. K. LINNEHAN, *Nature* **247** (1974) 220.
14. J. HU, J. J. RUSSELL, B. BEN-NISSAN and R. VAGO, *J. Mater. Sci. Lett.* **20** (2001) 85.
15. J. PENA, R. LEGEROS, R. ROHANIZADEH and J. LEGEROS, *Key Eng. Mater.* **192–195** (2001) 267.
16. R. A. WHITE, E. W. WHITE and R. J. NELSON, *Biomat. Med. Dev. Art. Org.* **7** (1979) 127.
17. A. MILEV, PhD thesis, University of Technology, Sydney, 2002.
18. F. BLOCH, *Phys. Rev.* **70** (1946) 460.
19. F. BLOCH, W. W. HAUSEN and M. PACKARD, *ibid.* **70** (1946) 474.
20. T. C. FARRAR and E. D. BECKER, "Pulse and Fourier Transform NMR" (Academic Press, New York, USA).
21. R. J. S. BROWN, *J. Magn. Reson.* **82** (1989) 539.
22. D. P. GALLEGOS and D. M. J. SMITH, *Coll. Interf. Sci.* **122** (1988) 143.
23. K. R. BROWNSTEIN and C. E. TARR, *Phys. Rev.* A **19** (1979) 2446.
24. M. G. PRAMMER, *Proc. Soc. Petrol. Engns.* **55** (1994) SPE 36980.
25. A. L. McCUTCHEON, W. A. BARTON and M. A. WILSON, *Energy and Fuels* **17** (2003) 107.
26. D. W. MARQUARDT, "Numerical Recipes" (Cambridge University Press, Cambridge, 1963).
27. J. C. NASH, *J. Soc. Industr. Appl. Mathem.* **11** (1979) 431.
28. A. SLOSARCZYK, E. STOBIERSKA and Z. PASZKIEWICZ, *J. Mater. Sci. Lett.* **18** (1999) 1163.

Received 26 August 2003
and accepted 29 April 2004